

MOMUSE: MOMENTUM MULTI-MODAL TARGET SPEAKER EXTRACTION FOR REAL-TIME SCENARIOS WITH IMPAIRED VISUAL CUES

Junjie Li¹, Ke Zhang², Shuai Wang², Kong Aik Lee¹, Haizhou Li^{2,3}

¹ Department of Electrical and Electronic Engineering, The Hong Kong Polytechnic University, Hong Kong

² Shenzhen Research Institute of Big Data, Shenzhen, China

³ School of Data Science, The Chinese University of Hong Kong, Shenzhen (CUHK-Shenzhen), China

ABSTRACT

Audio-visual Target Speaker Extraction (AV-TSE) aims to isolate the speech of a specific target speaker from an audio mixture using time-synchronized visual cues. In real-world scenarios, visual cues are not always available due to various impairments, which undermines the stability of AV-TSE. Despite this challenge, humans can maintain attentional momentum over time, even when the target speaker is not visible. In this paper, we introduce the *Momentum Multi-modal target Speaker Extraction* (MoMuSE), which retains a speaker identity momentum in memory, enabling the model to continuously track the target speaker. Designed for real-time inference, MoMuSE extracts the current speech window with guidance from both visual cues and dynamically updated speaker momentum. Experimental results demonstrate that MoMuSE exhibits significant improvement, particularly in scenarios with severe impairment of visual cues.¹

Index Terms— Audio-visual, Momentum, Multi-modal, Target Speaker Extraction, Visual Impairments

1. INTRODUCTION

Audio-visual Target Speaker Extraction (AV-TSE) [1–4] aims to extract the speech of target speaker with visual cues, such as lip or face image sequences, as references. Visual cues, known for their resilience against acoustic noise, have demonstrated superior performance compared to audio-only approaches [5–7] in complex acoustic environments.

Despite the significant benefits that visual information provides to the AV-TSE task, challenges arise when visual cues are temporarily unavailable in real-world scenarios, such as pose variations or the absence of the target person’s video [8]. Additionally, issues like lip occlusion or a low-quality camera [9] can result in unclear lip areas. These challenges dynamically disrupt the reliance of AV-TSE on time-aligned cue sequences.

Several related studies have tried to address the aforementioned challenges. Sadeghi and Alameda-Pineda [10, 11] proposed switching from an audio-visual variational auto-encoder (VAE) to an audio-only VAE when visual quality is poor. Wu et al. [12] incorporated an attention mechanism, selecting relevant visual features based on mixed audio features. In contrast to discarding low-quality visual features, Pan et al. [13] adopted an innovative approach by reconstructing corrupted video through audio-visual correspondence. Furthermore, the VS model [9] and the audio-visual SpeakerBeam [14, 15] learn a speaker embedding from pre-enrolled speech and rely

on this embedding when visual cues are unreliable. Liu et al. [16] propose a triple loss function, where visual cues are leveraged only during the training phase and are not directly fused into the model’s input features.

However, the aforementioned approaches introduce an additional step of using pre-enrollment, and the pre-enrolled speech may not align with the actual acoustic scenario during usage. Instead of pre-enrollment, we propose tracking speaker identity using speech derived from previous time steps, offering a more accurate representation of the speaker’s current vocal characteristics. While leveraging such “self-enrollment” speech for second-phase inference has proven effective in tasks like speech enhancement [17], audio-based speech separation [18–21], and target speaker extraction [22–25], the performance degrades if the self-enrollment speech is of poor quality.

In this paper, we propose the *Momentum Multi-modal target Speaker Extraction* (MoMuSE), a novel framework that employs a memory bank with a momentum mechanism to dynamically track and update the speaker’s identity using previous time steps. This dynamic updating ensures that the memory bank retains the most accurate speaker embedding, enabling MoMuSE to maintain focus on the target speaker during real-time inference, even when visual cues are corrupted or unavailable. Experiments demonstrate that our proposed MoMuSE achieves a momentum effect, enabling target speaker extraction to continue functioning even when visual cues are completely absent.

2. VISUAL IMPAIRMENTS

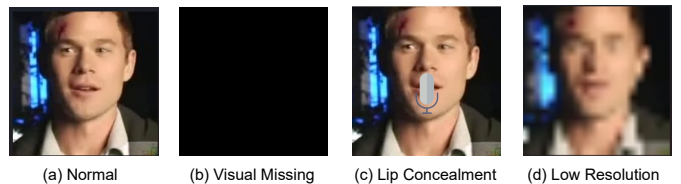


Fig. 1. Examples of normal and impaired visual frames.

The normal visual frame is depicted in Fig. 1 (a). However, in real-world scenarios, clear visual frames may not be available throughout entire conversations. As shown in Fig. 1, prevalent issues include: 1) **Visual Missing**, where the speaker’s face remains undetected; 2) **Lip Concealment**, where objects such as hands or microphones obscure the mouth region; and 3) **Low Resolution**,

¹Demo: https://mrjunjieli.github.io/demo_page/MoMuSE/index.html.
Code: <https://github.com/mrjunjieli/MoMuSE>.

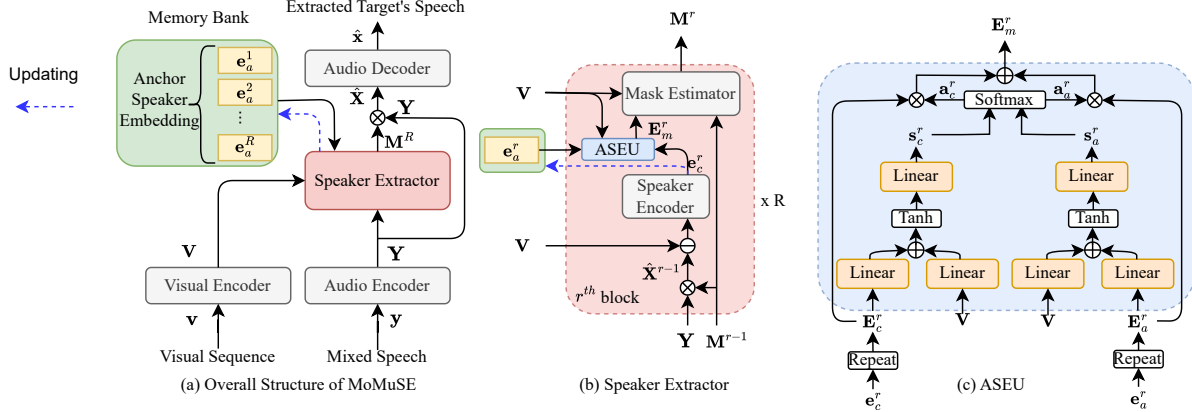


Fig. 2. (a) Overall structure of MoMuSE. Modules in gray denote the original structures from MuSE, while modules in other colors denote the proposed new structures. (b) Speaker Extractor. (c) The detailed structure of ASEU, which is an attention based module. \otimes , \ominus and \oplus refer to point-wise multiplication, concatenation and point-wise addition.

caused by inferior camera quality, the camera being out of focus, or the speaker’s distance from the camera.

3. PROPOSED METHOD

To enhance the stability of AV-TSE systems in the aforementioned impaired scenarios and avoid introducing a pre-enrollment process [26–29], we aim to leverage the advantages of dynamic visual frames when visual cues are reliable while incorporating alternative speaker voiceprint cue when visual information is impaired. In this paper, we introduce MoMuSE, a novel framework that employs a dynamically updated speaker momentum as an additional reference. MoMuSE enables robust speaker extraction even in the presence of visual impairments, presenting a more effective way to harness the complementary nature of visual and audio modalities.

3.1. Recap of MuSE

MuSE [30] is an AV-TSE model that utilizes visual cues and a self-enrolled speaker embedding as references. As depicted in Fig 2, the modules in gray represent the original MuSE structure, while the modules in other colors indicate our proposed new components.

MuSE consists of four main modules: an audio encoder, an audio decoder, a visual encoder, and a speaker extractor. The audio encoder transforms the time-domain mixed speech y into a latent representation \mathbf{Y} , and the audio decoder reconstructs the extracted target speech x from its latent representation $\hat{\mathbf{X}}$. The visual encoder processes the visual sequence \mathbf{v} to generate visual embeddings \mathbf{V} . The speaker extractor iteratively refines the quality of the extracted speech using R extractor blocks. Each extractor block includes a speaker encoder and a mask estimator, as illustrated in Fig 2 (b). The speaker encoder fuses the estimated speech representation $\hat{\mathbf{X}}^{r-1}$ and the visual representation \mathbf{V} to generate a speaker embedding \mathbf{e}_c^r . The mask estimator then generates a mask \mathbf{M}^r to isolate the target speech. Here, $r = (1, 2, \dots, R)$ indicates the index of the extractor block, with distinct parameter weights for each block.

In MuSE, the self-enrolled speaker embedding \mathbf{e}_c^r is derived from the current window of visual and audio representations, assuming the visual information is consistently reliable. However, this

assumption fails under visual impairments. Our proposed MoMuSE addresses this limitation by incorporating a dynamic speaker momentum mechanism. It leverages a memory bank to store historical information, updating embeddings based on a reliability assessment of the visual cues, thus enhancing stability even when visual inputs are absent.

3.2. MoMuSE architecture

MoMuSE shares a similar structure with MuSE, yet it incorporates a memory bank that allows it to leverage historical voiceprint information from previously extracted speech, as illustrated in Fig 2 (a). The memory bank comprises R anchor speaker embeddings, denoted as $\mathbf{e}_a^1, \dots, \mathbf{e}_a^R$, which store the historical voiceprint information of the target speaker. Here, the subscript a denotes “anchor”. In addition, to effectively combine historical and current speaker information, we propose an *Anchor Speaker Embedding Updating* (ASEU) sub-module within each speaker extractor block. This sub-module integrates historical embeddings into the extraction process for the current window, adapting based on the visual features’ quality in the current window. We implement the ASEU sub-module using an additive attention fusion mechanism inspired by [14, 31]², as shown in Fig 2 (c).

To maintain temporal resolution consistency, we apply temporal replication to the speaker embeddings³

$$\mathbf{E}_\psi \in \mathbb{R}^{H \times L} = \text{Repeat}(\mathbf{e}_\psi \in \mathbb{R}^{H \times 1}) \quad (1)$$

where H and L are the feature dimension and time length, respectively, and $\psi \in \{a, c\}$ denotes the specific type of embedding being used. Next, the attention mechanism computes two score vectors \mathbf{s}_c and \mathbf{s}_a for \mathbf{E}_c and \mathbf{E}_a , respectively:

$$\mathbf{s}_\psi = \text{Linear}(\text{Tanh}(\text{Linear}(\mathbf{E}_\psi) + \text{Linear}(\mathbf{V}))) \quad (2)$$

where $\mathbf{V} \in \mathbb{R}^{H \times L}$ represents the visual feature. These score vectors are then normalized using a softmax function to produce attention

²<https://github.com/sooftware/attentions/blob/master/attentions.py>

³For notational clarity, the superscript r denoting the r -th block will be neglected in Section 3.2 and Section 3.3.

weights:

$$\mathbf{a}_{\psi,l} = \frac{\exp(\mathbf{s}_{\psi,l})}{\exp(\mathbf{s}_{c,l}) + \exp(\mathbf{s}_{a,l})} \quad (l = 1, 2, \dots, L), \quad (3)$$

where l denotes the time step. Finally, the momentum-based speaker embedding sequence \mathbf{E}_m is computed by fusing \mathbf{E}_c and \mathbf{E}_a according to their attention weights:

$$\mathbf{E}_m = \mathbf{a}_c \otimes \mathbf{E}_c + \mathbf{a}_a \otimes \mathbf{E}_a, \quad (4)$$

where \otimes denotes point-wise multiplication. In theory, when the current visual feature \mathbf{V} is unreliable, the attention mechanism tends to assign lower weights to current speaker embedding sequence \mathbf{E}_c .

3.3. Momentum mechanism

In online real-time processing [23], the model begins processing only after the incoming mixed input speech accumulates to a pre-defined initialization length L_{init} (in seconds). Once this initialization is complete, the model processes the mixed speech y using a window size of L_{win} (in seconds), and then advances forward by a step size of L_{shift} (in seconds). In subsequent discussions, we refer to the t -th processing window as the (t) -th window step. At the t -th window step, the model takes the mixed speech $y(t)$ and the corresponding visual sequence $\mathbf{v}(t)$ as inputs, and outputs the estimated target speech $\hat{\mathbf{x}}(t)$:

$$\hat{\mathbf{x}}(t) = \text{MoMuSE}(\mathbf{y}(t), \mathbf{v}(t)) \quad (5)$$

The momentum mechanism is implemented in online scenarios and contains three components: **initialization**, **generation**, and **updating**.

Initialization: To maintain continuous attention on the target speaker in unreliable visual scenarios, the historical voiceprint information of the target speaker needs to be preserved. We introduce a memory bank to store this information. At the first window step (initialization), the memory bank is empty. The dimension of the mixed speech of current window is $\mathbf{y}(1) \in \mathbb{R}^{1 \times L_{\text{init}}}$. Given that the memory bank is initially empty, the ASEU sub-module is not utilized at this step. Instead, the current speaker embedding sequence $\mathbf{E}_c(1)$ is directly used as input to the mask estimator. Once the corresponding target speech is estimated, the memory bank is initialized with the current speaker embedding $\mathbf{e}_c(1)$:

$$\mathbf{e}_a = \mathbf{e}_c(1). \quad (6)$$

This initialization allows the memory bank to begin tracking the target speaker's voiceprint for subsequent processing steps.

Generation: In subsequent window steps ($t > 1$), MoMuSE leverages the ASEU sub-module to effectively balance the historical and current voiceprint information. Using the visual representation $\mathbf{V}(t)$ ⁴ as the key, the model generates a momentum-based speaker embedding sequence $\mathbf{E}_m(t)$.

The attention mechanism within the ASEU computes varying attention weights at each time step, dynamically adjusting the contribution of the current speaker embedding sequence $\mathbf{E}_c(t)$ and the historical anchor embedding sequence $\mathbf{E}_a(t)$. This process allows MoMuSE to adaptively fuse current and past voiceprint information, ensuring robust target speaker extraction even when visual features are impaired or unreliable

⁴ $\mathbf{V}(t)$ is the visual feature corresponding to the input visual sequence $\mathbf{v}(t)$.

Updating: To ensure only high-quality speaker representation is retained in the memory bank, updates are performed when a superior speaker embedding is detected. The average attention weights $\bar{\mathbf{a}}_c(t)$ is employed as the criterion to determine whether a memory update should be triggered:

$$\mathbf{e}_a = \begin{cases} \mathbf{e}_c(t) & \text{if } \bar{\mathbf{a}}_c(t) > \theta \text{ for } t = 2, 3, 4, \dots, T \\ \mathbf{e}_a & \text{otherwise,} \end{cases} \quad (7)$$

where $\bar{\mathbf{a}}_c(t) \in \mathbb{R}^1$ denotes the mean of the attention weights $\mathbf{a}_c(t)$ across the time dimension, and θ is a predefined threshold.

3.4. Loss function

Following MuSE [30], we use the scale-invariant signal-to-noise ratio (SI-SNR) loss [32] and cross-entropy (CE) loss:

$$\mathcal{L}_{\text{SI-SNR}}(\mathbf{x}, \hat{\mathbf{x}}) = -10 \log_{10} \frac{\left\| \frac{\langle \hat{\mathbf{x}}, \mathbf{x} \rangle \mathbf{x}}{\|\mathbf{x}\|^2} \right\|^2}{\|\hat{\mathbf{x}} - \frac{\langle \hat{\mathbf{x}}, \mathbf{x} \rangle \mathbf{x}}{\|\mathbf{x}\|^2}\|}, \quad (8)$$

$$\mathcal{L}_{\text{CE}}(\mathbf{e}_c^r) = -\sum_{n=1}^N d_n \log(\text{softmax}(\mathbf{W}^r \mathbf{e}_c^r)), \quad (9)$$

where d_n is class label for speaker n and \mathbf{x} is target speech. N is the number of speakers in dataset. \mathbf{W}^r is a learnable weight matrix in r -th block used to project speaker embedding \mathbf{e}_c^r to a one-hot class label.

Additionally, we propose a penalty loss on the attention weight \mathbf{a}_a^r , mitigating the model's excessive reliance on the anchor speaker embedding \mathbf{e}_a^r :

$$\mathcal{L}_{\text{pe}} = \sum_{r=1}^R \frac{\|\mathbf{a}_a^r\|_1}{L}. \quad (10)$$

Since the current speaker embedding \mathbf{e}_c^r is more relevant to the current speech utterance, we encourage the model to learn more from it, especially when \mathbf{e}_c^r is reliable.

3.5. Training procedure

In autoregressive training, the past extracted speech is used as input for the current extraction, which can significantly increase computational overhead if every sliding window is optimized. Drawing inspiration from the training settings in NeuroHeed [23], we propose a Segment-Level Optimization (**Seg**) strategy that simulates only the first two window steps during the training phase. This approach effectively reduces computational cost while still capturing the essence of the autoregressive process.

To further enhance model convergence, we introduce two additional strategies: Parameter Initialization (**PI**), which helps the model start with better initial weights, and Utterance-Level Optimization (**Utt**), which focuses on optimizing the model at the utterance level to refine overall performance.

PI: Before training MoMuSE, we initialize its parameters (excluding ASEU) using the checkpoint from the 50-th training epoch of MuSE.

Utt: MoMuSE processes the whole utterance of visual and audio inputs, ensuring the model encounters long data, which aims to improve the robustness of the speaker encoder:

$$\hat{\mathbf{x}}, \mathbf{e}_c^r = \text{MoMuSE}(\mathbf{y}, \mathbf{v}), \quad (11)$$

$$\mathcal{L}_{\text{utt}} = \mathcal{L}_{\text{SI-SNR}}(\mathbf{x}, \hat{\mathbf{x}}) + \lambda \sum_{r=1}^R \mathcal{L}_{\text{CE}}(\mathbf{e}_c^r), \quad (12)$$

where λ controls the contribution of \mathcal{L}_{CE} .

Seg. To simulate autoregressive training, the entire utterance is split into two segments. The extraction of the second segment incorporates past extracted speaker embedding as input. Following the settings in NeuroHeed [23], we define the window length $L_{win} \sim \mathcal{U}(1.05s, 3.2s)$, shift length $L_{shift} \sim \mathcal{U}(0.05s, 0.2s)$, and initialization length $L_{init} \sim \mathcal{U}(0.05s, 3s)$, where \mathcal{U} denotes a uniform distribution, and the unit is in seconds (s). In the first window step, MoMuSE processes the mixed audio and visual sequence from the first segment:

$$\hat{\mathbf{x}}(1), \mathbf{e}_c^r(1) = \text{MoMuSE}(\mathbf{y}(1), \mathbf{v}(1)). \quad (13)$$

The memory bank is initialized as per Eq. 6. In the subsequent window step, MoMuSE utilizes stored voiceprint information from the memory bank to estimate the second segment’s speech and generate momentum-based speaker embedding sequences:

$$\hat{\mathbf{x}}(2), \mathbf{E}_m^r(2) = \text{MoMuSE}(\mathbf{y}(2), \mathbf{v}(2), \mathbf{e}_a^r). \quad (14)$$

To enhance the accuracy of the momentum-based speaker embedding, we define the segment loss as:

$$\mathcal{L}_{seg} = \mathcal{L}_{SI-SNR}(\mathbf{x}(2), \hat{\mathbf{x}}(2)) + \lambda \sum_{r=1}^R \mathcal{L}_{CE}(\bar{\mathbf{E}}_m^r(2)), \quad (15)$$

where $\bar{\mathbf{E}}_m^r(2) \in \mathbb{R}^{H \times 1}$ is the mean of $\mathbf{E}_m^r(2)$ across the time dimension.

The total loss is designed as follows:

$$\mathcal{L}_{total} = \alpha \mathcal{L}_{utt} + \beta \mathcal{L}_{seg} + \gamma \mathcal{L}_{pe}, \quad (16)$$

where α , β , and γ are hyperparameters balancing the contribution of each loss component

4. EXPERIMENTAL DETAILS

4.1. Dataset

All the models were trained on the Voxceleb2 dataset [33], and the dataset simulation scripts in [30] were adopted to generate our dataset. The simulated 2-speaker mixed speech dataset contains 20k, 5k and 3k utterances for the training, validation and test sets, respectively. The Signal-to-Noise (SNR) ratio was randomly chosen from -10 to 10 dB. The videos were sampled at 25 FPS and the synchronized audio is sampled at 16 kHz. For each utterance, a random type of visual impairment from the set {visual missing, lip concealment, low resolution} was applied. The impairment ratio is randomly chosen from [0%, 80%) for the training and validation sets, and from [0%, 100%) for the test set.

4.2. Implementation details

The initial learning rate was set to $1e^{-3}$ when optimizing from scratch and $1e^{-4}$ when initialized from a pre-trained checkpoint, using the Adam optimizer. The learning rate is halved if the best validation loss (BVL) does not improve within six consecutive epochs, and the training stops if the BVL does not improve within ten consecutive epochs. The maximum number of training epochs is set to 100. We set θ to a relatively large value 0.7 to make sure \mathbf{e}_a^r is replaced only when \mathbf{e}_c^r is accurate enough. For online inference, we set L_{init} , L_{win} and L_{shift} to 1s, 2.7s and 0.2s, respectively, according to [23]. The hyperparameters α , β , γ , and λ are set to 0.3, 0.7, 0.05, and 0.1, respectively.

The SI-SNR loss is scale-invariant, meaning the energy of the estimated speech may vary across different window steps. To ensure consistent energy levels in the estimated speech, we apply the NeuroHeed normalization strategy [23] in inference.

5. RESULTS

5.1. Causal vs. non-causal

Table 1. SI-SNR (dB) of MuSE with different training settings.

Causal	Impaired	Training setting	Evaluation mode			
			Offline		Online	
			Normal	Impaired	Normal	Impaired
✗	✗ [30]	11.70	7.08	9.08	3.67	
✗	✓	10.11	11.30	8.74	6.05	
✓	✗	9.73	5.73	7.49	2.69	
✓	✓	9.34	8.26	7.20	4.69	

In this section, we explore the optimal training settings for online scenarios where visual cues are impaired. Table 1 demonstrates that the non-causal model configuration [32] outperforms the causal variant in both online and offline evaluation modes. Additionally, incorporating impaired video data into the training set significantly enhances performance in scenarios where visual cues are unreliable. However, this improvement comes at the cost of reduced performance when the visual inputs are normal. This trade-off likely occurs because the model learns to rely less on visual information when it is exposed to impaired visual data during training. The second row of Table 1, which employs a non-causal model and incorporates impaired data during training, shows the best performance in our target scenario, online inference with impaired visual cues. Therefore, this configuration is adopted in subsequent experiments to ensure optimal results.

5.2. Comparative analysis with baselines

Table 2. ‘V’ and ‘I’ denote visual sequences and static image, respectively. ‘Data’ denotes the number of utterances in training set.

Model	Cue	SI-SDR	SDR	PESQ	STOI	Data
FaceFilter [34]	I	-	2.5	-	-	2,000k
VisualVoice [1]	I	-	7.06	-	0.80	1,000k
MuSE	V	6.05	6.66	1.67	0.77	20k
MoMuSE	V	6.87	7.59	1.81	0.78	20k

We evaluate our proposed MoMuSE model and several baseline approaches using multiple performance metrics: Scale-Invariant Signal-to-Noise Ratio (SI-SNR), Signal-to-Distortion Ratio (SDR) [35], Perceptual Evaluation of Speech Quality (PESQ) [36], and Short-Time Objective Intelligibility (STOI) [37]. The results are summarized in Table 2.

First, compared to baselines that utilize a static image (I) as the visual cue (e.g., FaceFilter and VisualVoice), MuSE and MoMuSE leverage dynamic visual sequences (V), achieving comparable or even superior performance while requiring less training data.

This highlights the effectiveness of using time-varying visual features (such as lip movements) to enhance speech separation. Second, when visual cues are unreliable or absent, the use of historical voiceprint stored in memory bank as complementary information boosts performance. MoMuSE outperforms MuSE across all evaluation metrics, showing its robustness in real-world scenarios with impaired visual cues.

5.3. Ablation studies

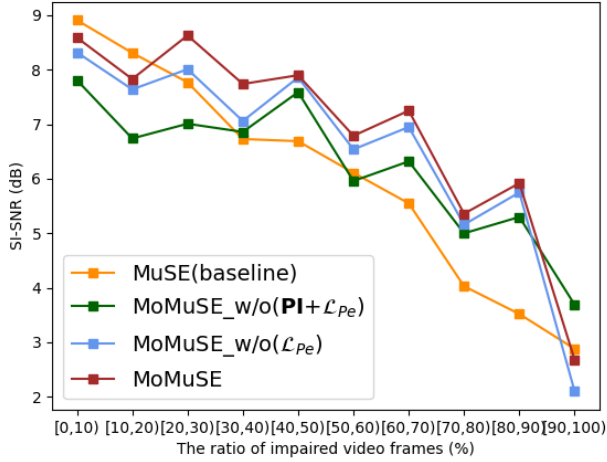


Fig. 3. Model performance under varied impaired ratios is shown, where MoMuSE_w/o(PI+LPe) excludes parameter initialization (PI) and penalty loss (\mathcal{L}_{Pe}), and MoMuSE_w/o(\mathcal{L}_{Pe}) excludes only \mathcal{L}_{Pe} .

Fig.3 illustrates the impact of different training strategies on model performance across varying levels of visual impairment. Compared to MoMuSE_w/o(\mathcal{L}_{Pe}), MoMuSE demonstrates improved performance across all scenarios, highlighting the importance of the \mathcal{L}_{Pe} loss. By prioritizing the current speaker embedding \mathbf{e}_c^r , this loss function ensures more discriminative and effective representations, particularly in scenarios with inconsistent or absent visual cues.

Table 3. Comparative analysis of various types of impairments.

Impairments	Model	SI-SNR	SDR	PESQ	STOI
Visual Missing	MuSE	3.46	4.19	1.53	0.71
	MoMuSE	6.13	6.92	1.79	0.76
Lip Concealment	MuSE	7.32	7.88	1.73	0.80
	MoMuSE	7.08	7.78	1.81	0.78
Low Resolution	MuSE	7.37	7.92	1.75	0.80
	MoMuSE	7.39	8.06	1.84	0.79

Additionally, the Parameter Initialization (PI) strategy further enhances performance by initializing the model with pre-trained parameters, which strengthens the quality of learned embeddings and improves adaptability to varying impairment levels. MoMuSE also outperforms MuSE, especially in high visual impairment scenarios (over 20%), by effectively leveraging historical voiceprint information as a fallback when visual cues are unreliable. However, a slight performance drop is observed in low impairment scenarios, likely due to reduced reliance on visual cues.

Although MoMuSE exhibits strong overall performance, its effectiveness decreases as the impairment ratio increases, suggesting that visual cues remain more reliable than voiceprint-based information when both modalities are available.

5.4. Impact of the impairment types

Table 3 presents the performance of MoMuSE and MuSE on three types of visual impairments. In scenarios of complete visual absence, where no useful visual information is available, MoMuSE shows clear effectiveness, highlighting its ability to excel when visual cues are severely compromised. This result underscores the model's strength in leveraging momentum-based speaker embeddings to maintain robust performance. For cases of lip concealment and low resolution, although MoMuSE does not exhibit significant improvements, its performance remains competitive, suggesting that even with partial visual impairments, the model can effectively utilize available cues while relying on speaker momentum for stability.

5.5. Analyzing total visual absence

Table 4. Comparative analysis on total visual absence. The performance of models on different utterance lengths.

	[0s, 5s)	[5s, 10s)	[10s, 15s)	[15s, 20s)	[20s, ∞)
MuSE	3.44	1.23	-1.38	-0.90	-6.81
MoMuSE	7.24	7.81	7.69	10.88	12.25

In this section, we evaluate the model's performance in a challenging scenario where visual cues are available only during the initialization step (the 1st second) and are entirely absent in subsequent steps.

Table 4 presents the SI-SNR (dB) performance of models with varying utterance lengths. First, MoMuSE consistently outperforms MuSE, demonstrating its ability to maintain focus on the target speaker over time in the absence of visual cues. Second, as the length of the utterance increases, MoMuSE shows improved performance. This improvement can be attributed to its updating mechanism, which discards poorer speaker embeddings and retains more reliable ones in the memory bank during inference. Using these better speaker embeddings, MoMuSE is able to achieve enhanced performance.

An interesting observation is MoMuSE's performance in Table 4 exceeds its performance in Table 3. We attribute this to the clean visual input during the initialization step in Table 4, whereas impaired visuals might occur in the initialization step in Table 3. This highlights the critical importance of having clean visuals during the initialization step.

6. CONCLUSION AND FUTURE WORK

We have proposed the MoMuSE, an extension of the MuSE model with a momentum mechanism, to track the target speaker in AV-TSE tasks even when visual cues are impaired or missing. Our approach uses a built-in memory bank to maintain the target speaker's hidden state, eliminating the need for audio pre-enrollment. In the future, we will focus on refining the confidence mechanism and memory bank design to adapt to diverse scenarios.

7. REFERENCES

[1] Ruohan Gao and Kristen Grauman, “Visualvoice: Audio-visual speech separation with cross-modal consistency,” in *2021 IEEE/CVF Conference on Computer Vision and Pattern Recognition (CVPR)*. IEEE, 2021, pp. 15490–15500.

[2] Ariel Ephrat, Inbar Mosseri, Oran Lang, Tali Dekel, Kevin Wilson, Avinatan Hassidim, William T. Freeman, and Michael Rubinstein, “Looking to listen at the cocktail party: a speaker-independent audio-visual model for speech separation,” *ACM Trans. Graph.*, vol. 37, no. 4, 2018.

[3] Junjie Li, Ruijie Tao, Zexu Pan, Meng Ge, Shuai Wang, and Haizhou Li, “Audio-visual active speaker extraction for sparsely overlapped multi-talker speech,” in *ICASSP 2024-2024 IEEE International Conference on Acoustics, Speech and Signal Processing (ICASSP)*. IEEE, 2024, pp. 10666–10670.

[4] Ruijie Tao, Xinyuan Qian, Yidi Jiang, Junjie Li, Jiadong Wang, and Haizhou Li, “Audio-visual target speaker extraction with reverse selective auditory attention,” *arXiv preprint arXiv:2404.18501*, 2024.

[5] Triantafyllos Afouras, Joon Son Chung, Andrew Senior, Oriol Vinyals, and Andrew Zisserman, “Deep audio-visual speech recognition,” *TPAMI*, 2018.

[6] Wupeng Wang, Chao Xing, Dong Wang, Xiao Chen, and Fengyu Sun, “A robust audio-visual speech enhancement model,” in *ICASSP*. IEEE, 2020, pp. 7529–7533.

[7] Vahid Ahmadi Kalkhorani, Anurag Kumar, Ke Tan, Buye Xu, and DeLiang Wang, “Audiovisual speaker separation with full- and sub-band modeling in the time-frequency domain,” in *ICASSP 2024 - 2024 IEEE International Conference on Acoustics, Speech and Signal Processing (ICASSP)*, 2024, pp. 12001–12005.

[8] Muhtahir O Oloyede, Gerhard P Hancke, and Hermanus C Myburgh, “A review on face recognition systems: recent approaches and challenges,” *Multimedia Tools and Applications*, vol. 79, pp. 27891–27922, 2020.

[9] Triantafyllos Afouras, Joon Son Chung, and Andrew Zisserman, “My Lips Are Concealed: Audio-Visual Speech Enhancement Through Obstructions,” in *Proc. Interspeech 2019*, 2019, pp. 4295–4299.

[10] Mostafa Sadeghi and Xavier Alameda-Pineda, “Switching variational auto-encoders for noise-agnostic audio-visual speech enhancement,” in *ICASSP 2021-2021 IEEE International Conference on Acoustics, Speech and Signal Processing (ICASSP)*. IEEE, 2021, pp. 6663–6667.

[11] Mostafa Sadeghi and Xavier Alameda-Pineda, “Robust unsupervised audio-visual speech enhancement using a mixture of variational autoencoders,” in *ICASSP 2020-2020 IEEE International Conference on Acoustics, Speech and Signal Processing (ICASSP)*. IEEE, 2020, pp. 7534–7538.

[12] Yifei Wu, Chenda Li, Jinfeng Bai, Zhongqin Wu, and Yanmin Qian, “Time-domain audio-visual speech separation on low quality videos,” in *ICASSP 2022-2022 IEEE International Conference on Acoustics, Speech and Signal Processing (ICASSP)*. IEEE, 2022, pp. 256–260.

[13] Zexu Pan, Wupeng Wang, Marvin Borsdorf, and Haizhou Li, “Imaginenet: Target speaker extraction with intermittent visual cue through embedding inpainting,” in *ICASSP 2023-2023 IEEE International Conference on Acoustics, Speech and Signal Processing (ICASSP)*. IEEE, 2023, pp. 1–5.

[14] Hiroshi Sato, Tsubasa Ochiai, Keisuke Kinoshita, Marc Delcroix, Tomohiro Nakatani, and Shoko Araki, “Multimodal attention fusion for target speaker extraction,” in *2021 IEEE Spoken Language Technology Workshop (SLT)*. IEEE, 2021, pp. 778–784.

[15] Tsubasa Ochiai, Marc Delcroix, Keisuke Kinoshita, Atsunori Ogawa, and Tomohiro Nakatani, “Multimodal speakerbeam: Single channel target speech extraction with audio-visual speaker clues,” in *INTERSPEECH*, 2019, pp. 2718–2722.

[16] Yinggang Liu, Yuanjie Deng, and Ying Wei, “A two-stage audio-visual speech separation method without visual signals for testing and tuples loss with dynamic margin,” *IEEE Journal of Selected Topics in Signal Processing*, vol. 18, no. 3, pp. 459–472, 2024.

[17] Pavel Andreev, Nicholas Babaev, Azat Saginbaev, Ivan Shchekotov, and Aibek Alanov, “Iterative autoregression: a novel trick to improve your low-latency speech enhancement model,” in *INTERSPEECH 2023*, 2023, pp. 2448–2452.

[18] Hui Wang, Yan Song, Zeng-Xi Li, Ian McLoughlin, and Li-Rong Dai, “An online speaker-aware speech separation approach based on time-domain representation,” in *ICASSP 2020-2020 IEEE International Conference on Acoustics, Speech and Signal Processing (ICASSP)*. IEEE, 2020, pp. 6379–6383.

[19] Zeng-Xi Li, Yan Song, Li-Rong Dai, and Ian McLoughlin, “Source-aware context network for single-channel multi-speaker speech separation,” in *2018 IEEE International Conference on Acoustics, Speech and Signal Processing (ICASSP)*. IEEE, 2018, pp. 681–685.

[20] Zeng-Xi Li, Yan Song, Li-Rong Dai, and Ian McLoughlin, “Listening and grouping: an online autoregressive approach for monaural speech separation,” *IEEE/ACM Transactions on Audio, Speech, and Language Processing*, vol. 27, no. 4, pp. 692–703, 2019.

[21] Zexu Pan, Gordon Wichern, François G. Germain, Kohei Saito, and Jonathan Le Roux, “Paris: Pseudo-autoregressive siamese training for online speech separation,” in *Interspeech 2024*, 2024, pp. 582–586.

[22] Chengyun Deng, Shiqian Ma, Yongtao Sha, Yi Zhang, Hui Zhang, Hui Song, and Fei Wang, “Robust Speaker Extraction Network Based on Iterative Refined Adaptation,” in *Proc. Interspeech 2021*, 2021, pp. 3530–3534.

[23] Zexu Pan, Marvin Borsdorf, Siqi Cai, Tanja Schultz, and Haizhou Li, “Neuroheed: Neuro-steered speaker extraction using eeg signals,” *IEEE/ACM Transactions on Audio, Speech, and Language Processing*, 2024.

[24] Ashutosh Pandey and DeLiang Wang, “Attentive training: A new training framework for speech enhancement,” *IEEE/ACM Transactions on Audio, Speech, and Language Processing*, vol. 31, pp. 1360–1370, 2023.

[25] Yiwen Wang, Zeyu Yuan, and Xihong Wu, “Dense: Dynamic embedding causal target speech extraction,” *arXiv preprint arXiv:2409.06136*, 2024.

[26] Xue Yang, Changchun Bao, Jing Zhou, and Xianhong Chen, “Target speaker extraction by directly exploiting contextual information in the time-frequency domain,” in *ICASSP 2024 -*

2024 IEEE International Conference on Acoustics, Speech and Signal Processing (ICASSP), 2024, pp. 10476–10480.

- [27] Xue Yang, Changchun Bao, and Xianhong Chen, “Coarse-to-fine target speaker extraction based on contextual information exploitation,” *IEEE/ACM Transactions on Audio, Speech, and Language Processing*, vol. 32, pp. 3795–3810, 2024.
- [28] Shuai Wang, Ke Zhang, Shaoxiong Lin, Junjie Li, Xuefei Wang, Meng Ge, Jianwei Yu, Yanmin Qian, and Haizhou Li, “Wesep: A scalable and flexible toolkit towards generalizable target speaker extraction,” in *Proc. Interspeech 2024*, 2024, pp. 4273–4277.
- [29] Ke Zhang, Junjie Li, Shuai Wang, Yangjie Wei, Yi Wang, Yannan Wang, and Haizhou Li, “Multi-level speaker representation for target speaker extraction,” *arXiv preprint arXiv:2410.16059*, 2024.
- [30] Zexu Pan, Ruijie Tao, Chenglin Xu, and Haizhou Li, “Muse: Multi-modal target speaker extraction with visual cues,” in *ICASSP 2021-2021 IEEE International Conference on Acoustics, Speech and Signal Processing (ICASSP)*. IEEE, 2021, pp. 6678–6682.
- [31] Dzmitry Bahdanau, Kyunghyun Cho, and Yoshua Bengio, “Neural machine translation by jointly learning to align and translate,” in *3rd International Conference on Learning Representations, ICLR 2015*, 2015.
- [32] Yi Luo and Nima Mesgarani, “Conv-tasnet: Surpassing ideal time–frequency magnitude masking for speech separation,” *IEEE/ACM transactions on audio, speech, and language processing*, vol. 27, no. 8, pp. 1256–1266, 2019.
- [33] Joon Son Chung, Arsha Nagrani, and Andrew Zisserman, “VoxCeleb2: Deep Speaker Recognition,” in *Proc. Interspeech 2018*, 2018, pp. 1086–1090.
- [34] Soo-Whan Chung, Soyeon Choe, Joon Son Chung, and Hong-Goo Kang, “FaceFilter: Audio-Visual Speech Separation Using Still Images,” in *Proc. Interspeech 2020*, 2020, pp. 3481–3485.
- [35] Emmanuel Vincent, Rémi Gribonval, and Cédric Févotte, “Performance measurement in blind audio source separation,” *IEEE transactions on audio, speech, and language processing*, vol. 14, no. 4, pp. 1462–1469, 2006.
- [36] Antony W Rix, John G Beerends, Michael P Hollier, and Andries P Hekstra, “Perceptual evaluation of speech quality (pesq)-a new method for speech quality assessment of telephone networks and codecs,” in *2001 IEEE international conference on acoustics, speech, and signal processing. Proceedings (Cat. No. 01CH37221)*. IEEE, 2001, vol. 2, pp. 749–752.
- [37] Cees H Taal, Richard C Hendriks, Richard Heusdens, and Jesper Jensen, “An algorithm for intelligibility prediction of time–frequency weighted noisy speech,” *IEEE Transactions on Audio, Speech, and Language Processing*, vol. 19, no. 7, pp. 2125–2136, 2011.